Divergent Roles of Hepatitis B Virus X-Associated Protein 2 (XAP2) in Human versus Mouse Ah Receptor Complexes[†]

Preeti Ramadoss,[§,#,‡] John R. Petrulis,[§,#] Brett D. Hollingshead,[#,‡] Ann Kusnadi,[#] and Gary H. Perdew*[,#]

Center for Molecular Toxicology and Carcinogenesis and the Department of Veterinary Science and Graduate Program in Biochemistry and Molecular Biology, The Pennsylvania State University, University Park, Pennsylvania 16802

Received October 8, 2003; Revised Manuscript Received November 20, 2003

ABSTRACT: The aryl hydrocarbon receptor (AhR) mediates the toxicologic and carcinogenic properties of 2,3,7,8-tetrachlorodibenzo-*p*-dioxin. In the cytoplasm, the AhR is complexed with a dimer of hsp90, and the hepatitis B virus X-associated protein 2 (XAP2). Most studies that have examined the ability of XAP2 to modulate the AhR have characterized the mouse receptor (mAhR). However, the amino acid sequence of mAhR is significantly different from human AhR (hAhR) in the carboxy terminal half of the protein, and this could lead to differences in the behavior of the two receptors. mAhR−yellow fluorescent protein (YFP) and hAhR−YFP were used to compare nucleocytoplasmic shuttling properties and the ability of XAP2 to modulate their activity. As reported previously, mAhR localized predominantly in the nucleus and was redistributed to the cytoplasm by coexpression of XAP2 in COS-1 cells. Leptomycin B treatment revealed that XAP2 blocked mAhR−YFP translocation to the nucleus in the absence of ligand. In contrast, hAhR−YFP localized predominantly in the cytoplasm, and coexpression of XAP2 did not affect this localization, and did not block nuclear accumulation in the presence of leptomycin B. An XAP2 fusion protein with a nuclear localization signal fused to the carboxy terminus (XAP2−NLS) was utilized to test whether this protein could drag the AhR into the nucleus. Coexpression of mAhR−YFP and XAP2−NLS caused cytoplasmic localization of the mAhR, while hAhR−YFP was partially localized in the nucleus, suggesting that XAP2 remains bound to the hAhR during nucleocytoplasmic shuttling. The presence of XAP2 in the ligand-bound hAhR complex enhanced the rate of nuclear translocation but repressed transcriptional activity. Together, these results suggest that the hAhR differs biochemically from the mAhR.

2,3,7,8-Tetrachlorodibenzo-*p*-dioxin (TCDD)[1] exposure results in a wide range of toxicologic properties, including wasting syndrome, chloracne, tumor promotion, developmental defects such as cleft palate, and reproductive defects (*1*). TCDD is a prototypic ligand for the aryl hydrocarbon receptor. The AhR is a ligand-activated member of the bHLH−PAS transcription factor family that mediates essentially all of the toxic effects of dioxin (*2*). Members of this family include HIF1α, EPAS, and MOP3, which are involved in hypoxia, vascular remodeling, and circadian rhythm, respectively (*3*). Disruption of AhR gene expression in mice leads to smaller livers, reduced fecundity, and decreased body weight, indicating an important role for the AhR in normal metabolism (*4*). The mechanism for the decreased liver size appears to be due to smaller hepatocytes, which is probably due to portosystemic shunting of blood and persistent fetal vascular structures (*5*). The unliganded AhR exists as a tetrameric core complex, consisting of a ligand binding subunit, a dimer of hsp90, and XAP2 (as reviewed in ref *6*). Upon binding ligand, the cytosolic AhR translocates to the nucleus and interacts with the Ah receptor nuclear translocator protein, and the heterodimer regulates gene transcription by binding to dioxin response elements upstream of the transcription start site (*7*). Some of the known target genes of the AhR include CYP1A1, CYP1B1, UGT-1, and the GST-Ya subunit (*8*−*11*). However, the key target genes that are involved in toxicity are not known.

XAP2 shares high sequence homology with FKBP52 (an immunophilin that is complexed with the glucocorticoid receptor), but XAP2 appears to interact in a unique manner with the Ah receptor complex (*12*−*14*). The chaperone protein hsp90 appears to be required for the proper folding of the AhR into a high affinity ligand binding conformation and also stabilizes the receptor in the cytoplasm (*15*−*17*). XAP2 binds to both hsp90 and the receptor, which leads to enhanced stability of the complex (*18*). Transiently expressed mouse AhR is predominantly nuclear in COS-1 cells, while coexpression of mAhR with XAP2 leads to cytoplasmic localization of mAhR (*19*−*21*). The AhR has both a bipartite nuclear localization signal and a nuclear export signal, which

[†] This work was supported by National Institutes of Health NIEHS Grant ES04869.

* Corresponding author: Gary H. Perdew, Phone: (814) 865-0400. Fax: (814) 863-1696. E-mail: ghp2@psu.edu.

[§] These authors contributed equally to this paper.

[#] Center for Molecular Toxicology and Carcinogenesis and the Department of Veterinary Science.

[‡] Graduate Program in Biochemistry and Molecular Biology.

[1] TCDD: 2,3,7,8-tetrachlorodibenzo-*p*-dioxin, AhR: aryl hydrocarbon receptor, Hsp90: 90 kDa heat shock protein, XAP2: hepatitis B virus X-associated protein 2, ARNT: AhR nuclear translocator, mAhR: murine AhR, NLS: nuclear localization signal, NES: nuclear export signal, YFP: yellow fluorescent protein hAhR: human AhR, LMB: leptomycin B, MENG: 25 mM MOPS/2 mM EDTA/0.02% NaN_3/10% glycerol, TSDS−PAGE: tricine-sodium dodecyl sulfate−polyacrylamide gel electrophoresis, DTT: dithiothreitol.

10.1021/bi035827v CCC: $27.50
Published on Web 12/31/2003

enables the receptor to undergo rapid nucleocytoplasmic shuttling (*22*−*24*). High levels of XAP2 are capable of blocking ligand independent nuclear uptake (such as during the process of shuttling), suggesting that XAP2 sequesters the mAhR complex in the cytoplasm (*25*). However, the precise role(s) of XAP2 in the AhR complex remain(s) to be elucidated.

The majority of studies examining the biochemical properties of the AhR have been performed using the AhR from C57BL/6J mice. Interestingly, there are four distinct alleles found in various mouse strains, Ah^{b-1}, Ah^{b-2}, Ah^{b-3}, and Ah^{d} (*26*, *27*). The Ah^{b-1} allele that is found in C57BL/6J mice is most commonly studied and was used in the current study to compare mAhR to hAhR. It is not yet known which allele of the mAhR is most similar to the hAhR in terms of structure or behavior. However, the Ah^{d} allele is probably most similar to the hAhR in terms of ligand binding. The molecular weight of the AhR varies from 140 to 95 kDa between vertebrate species (*2*, *28*−*30*). In addition, the amino acid sequence of the AhR is not very well conserved across species, particularly in the carboxyl terminal half of the protein. For example, the hamster AhR has an expanded and degenerate transactivation domain compared to the human AhR, and they share only 51% homology (*29*). The question that needs to be addressed is whether this sequence degeneracy leads to a significant alteration in the biochemical activity of the AhR. In this report, a comparison was made of XAP2's ability to modulate the human AhR's biochemical properties versus the mAhRs biochemical properties. We show that XAP2 affects the expression level and cellular localization of mAhR, but not of hAhR, and this difference may be accounted for in part by the fact that the hAhR complex may have less XAP2 bound to it than the mAhR complex. These studies also demonstrate that XAP2 does not hinder β-importin binding by hAhR, whereas it has previously been shown that XAP2 hinders β-importin binding by mAhR (*25*). Finally, XAP2 appears to be present in the hAhR complex that shuttles into the nucleus in both its ligand-free and ligand-bound states, but not in the ligand-free or ligand-bound mAhR complex.

EXPERIMENTAL PROCEDURES

Construction and Sources of Expression Vectors. pcDNA3/βmAhR was used for expression of the mAhR (*31*). pCI/XAP2, pEFV5/hAhR, and pEYFP/mAhR were generated previously (*14*, *19*, *32*). pEYFP/hAhR was generated by inserting hAhR (amplified by PCR from pCI/hAhR with Xho1 and Xma1 sites added to enable ligation in frame with YFP) into the Xho1 and Xma1 restriction sites in the multiple cloning site of pEYFP−N1. The NLS mutant receptors pEYFP/mAhR/K13A, pEYFP/hAhR/K14A, pEYFP/hAhR/KRR14−16AAA, as well as pCI/hAhR/FLAG/KRR14−16AAA were generated using the Quickchange Site-Directed Mutagenesis kit (Stratagene, La Jolla, CA) with HPLC purified primers (Operon Technologies Inc., Alameda, CA and MWG Biotech, High Point, NC). The NLS deletion construct pEYFP/hAhR/Δ37−42, where the second half of the bipartite NLS is deleted, was generated using two primers by the method described in ref *33*. pCI/XAP2/FLAG/NLS was generated by the addition of the oligonucleotide sequence corresponding to the amino acid sequence KKK-RKRKK to the 3′ end of XAP2/FLAG cDNA, using standard PCR techniques. This amino acid sequence was derived from the NLS of lymphoid enhancer factor (*34*) and the first lysine in the derived sequence is from the FLAG sequence of XAP2−FLAG.

Cell Culture and Transient Transfection. Cells were grown in α-minimal essential medium supplemented with 10% fetal bovine serum (Hyclone Labs, Logan, UT), 100 IU/mL penicillin, and 0.1 mg/mL streptomycin (Sigma, St. Louis, MO) at 37 °C in 95% air, 5% CO_2. Transient transfections were accomplished using LipofectAMINE with PLUS Reagent (Invitrogen, Carlsbad, CA). COS-1 cells in 100-mm dishes received 9 μg of DNA with 30 μL of LipofectAMINE and 20 μL of PLUS reagent, while cells in six-well microplates received 1.5 μg of DNA with 5 μL of LipofectAMINE and 3.3 μL of PLUS reagent, according to the manufacturer's instructions.

Immunoprecipitations and Western Blotting. YFP-tagged proteins were immunoprecipitated using anti-GFP antibody (BD Biosciences, formerly Clontech, Palo Alto, CA) bound to protein G-sepharose (Pierce, Rockford, IL) or goat anti-rabbit IgG agarose (Sigma, St. Louis, MO). FLAG-tagged proteins were immunoprecipitated using anti-FLAG M2 agarose (Sigma). Immunoprecipitations were carried out in IP buffer (MENG with 20 mM MoO_4^{2-}, 50 mM NaCl, 2 mg/mL bovine serum albumin, 2 mg/mL ovalbumin) and washed in wash buffer (MENG with 20 mM MoO_4^{2-} and 50 mM NaCl), resolved by TSDS−PAGE and blotted to PVDF membrane (Millipore, Bedford, MA) as previously described (*35*). Bands were visualized by Western blot analysis using for AhR: RPT1 MAb (*36*), for hsp90: anti-hsp84/86 rabbit polyclonal Abs (*37*), for XAP2: anti-ARA9 MAb (Novus Biologicals, Littleton, CO), for p23: JJ5 MAb, from Dr. David Toft. Primary antibodies were detected with peroxidase conjugated goat anti-mouse IgG (GAM-P) or peroxidase conjugated donkey anti-rabbit polyclonal Abs (DAR−P) (Jackson Immunoresearch, West Grove, PA) and visualized using the Vector VIP substrate kit (Vector Laboratories Inc., Burlingame, CA). Primary antibodies were also visualized using ^{125}I-goat anti-mouse (Amersham Biosciences, Piscataway, NJ) in some experiments. Band intensities were quantitated by phosphorimage analysis.

Fluorescence Microscopy. For microscopy experiments, COS-1 cells in six-well plates or 35-mm glass bottom dishes (MatTek Corporation, Ashland, MA) were transfected with 0.75 μg of each receptor construct and 0.75 μg of either pEFV5 (control vector) or pCI/XAP2. Fluorescence micrographs were directly obtained from live cells with a SPOT RT Color model 2.2.0 cooled CCD camera fitted to a Nikon Eclipse TE300 inverted microscope with a Nikon Pan Fluor 60× objective or a Nikon Plan Apo 60X oil immersion lens. Leptomycin B (Sigma) was used to block nuclear export at a concentration of 10 nM for the indicated time.

Localization Scoring. COS-1 cells were transfected with 0.75 μg of pEYFP/hAhR without or with 0.75 μg of pCI/XAP2, using LipofectAMINE-PLUS. Cells were visualized by fluorescence microscopy and scored. Approximately 150 cells were scored per transfected well, and the percentage of fluorescent cells that showed either cytoplasmic or nuclear localization was plotted.

XAP2−NLS Localization Experiment. COS-1 cells in 100-mm dishes were transfected with 3 μg of pCI/XAP2 or pCI/XAP2/FLAG/NLS using LipofectAMINE-PLUS according

to the manufacturer's directions. Cells were harvested approximately 22 h post-transfection and resuspended in MENG + protease inhibitors. Cells were dounce homogenized on ice (35 strokes) and the lysate was centrifuged at 1000*g* for 20 min at 4 °C. The supernatant was saved to make cytosolic extract and the pellet (crude nuclei) was washed once with MENG and centrifuged again at 1000*g* for 10 min at 4 °C. The crude nuclei were then resuspended in 100 μL of MENG + 500 mM NaCl + protease inhibitors and incubated on ice for 1 h. The crude nuclear and cytosolic extracts were centrifuged at 100000*g* for 45 min at 4 °C. The supernatants were transferred to fresh tubes, and protein concentrations were estimated using BCA Protein Assay reagents (Pierce, Rockford, IL). A total of 75 μg of proteins from each extract were resolved by TSDS−PAGE, transferred to PVDF membrane, and analyzed by Western blot as described earlier.

Importin/AhR Interaction Assay. COS-1 cells in 100-mm dishes were transfected with either pCI/hAhR/FLAG, or pCI/hAhR/FLAG and pCI/XAP2, or pCI/hAhR/FLAG/KRR14−16AAA (as an importin specificity control) using the LipofectAMINE-PLUS transfection method as described by the manufacturer. After 24 h, cells were trypsinized and washed three times with PBS. Cells from each set of three plates were lysed in 1 mL of MENG containing 20 mM $NaMoO_4$, 1% NP40, protease inhibitor cocktail (Sigma) and 1 mM DTT for 15 min at 4 °C, and centrifuged at 100000*g* for 30 min at 4 °C. The lysate (∼350 μL) was treated with TCDD to a final concentration of 10 nM or DMSO for 30 min at ambient temperature, followed by 10 min on ice. To the TCDD- or DMSO-treated lysate, 350 μL of immunoprecipitation buffer (MENG containing 20 mM $NaMoO_4$, 300 mM NaCl, 10 mg/mL BSA, 5 mg/mL ovalbumin, 1 mM DTT) was added and then transferred to 25 μL of prewashed anti-FLAG M2-agarose. The immunoprecipitations were incubated with agitation for 1 h at 4 °C and washed 3 times with MENG containing 100 mM NaCl and 20 mM $NaMoO_4$. The FLAG-tagged proteins were displaced by incubating with 200 μg of FLAG peptide (Sigma) in 125 μL of 50 mM Tris-HCl pH 7.5 containing 150 mM NaCl and 0.1% NP40 for 15 min at ambient temperature. The displacement was repeated once more, and supernatants were pooled. Each of the displaced FLAG-tagged proteins (200 μL) was transferred into 200 μL of importin-binding buffer (PBS containing 10 mg/mL BSA, 5 mg/mL ovalbumin, 0.2% NP40, 10% glycerol, and 1 mM DTT), and 22 μg of GST-importin β was added. GST-importin β was bacterially expressed and purified using glutathione-sepharose. The mixture was incubated for 30 min on ice, transferred to 25 μL of prewashed glutathione-Sepharose (Amersham Biosciences, Piscataway, NJ), incubated with agitation for 1 h at 4 °C, and washed 3 times with 1 mL of PBS. GST-importin β was displaced from the resin by incubating with 80 μL of 20 mM glutathione in 50 mM Tris-HCl pH 7.5 + 1 mM DTT for 5 min at ambient temperature. The displacement was repeated once more, and the pooled supernatant was subjected to Tricine SDS−PAGE. Protein was transferred onto PVDF membrane as previously described. The mAhR, XAP2, and GST-importin β were visualized by protein blot analysis using mAb RPT1, mAb anti-ARA9, and mAb B-14 anti-GST (Santa Cruz Biotechnology, Inc., Santa Cruz, CA), respectively. Primary antibodies were detected with ^{125}I-goat anti-mouse IgG, visualized by autoradiography, and band intensities were quantitated using phosphorimaging and/or gamma counting.

Luciferase Reporter Gene Assay. For the reporter assay testing the transcriptional activity of hAhR−YFP, COS-1 cells grown in six-well culture dishes were transfected using LipofectAMINE-PLUS according to the manufacturer's instructions. Each transfection included 100 ng of DRE-driven luciferase reporter construct pGudLuc 6.1, 100 ng of pCMV/β-gal, 50 ng of AhR construct (or control), and control vector (pEFV5), for a total of 1.5 μg of DNA per well. The day following transfection, cells were treated with 10 nM TCDD or DMSO (vehicle) for 8 h and then lysed. Luciferase activity was assayed using a Turner TD-20e luminometer with a luciferase assay system (Promega, Madison, WI), and luciferase readings were normalized to β-gal activity. To study XAP2 mediated repression of hAhR, COS-1 cells in six-well plates were transfected using LipofectAMINE-PLUS. Transfections were performed with a total of 1.5 μg of DNA per well, which included 50 ng of pCI/hAhR, 100 ng of pGudLuc6.1 and 200 ng of pCI/XAP2 where indicated. Cells were dosed for 7.5 h with 5 nM TCDD, lysed, and assayed for luciferase activity as described above. Luciferase readings were normalized to protein concentrations in each sample. Protein concentrations were estimated using BCA Protein Assay reagents (Pierce).

RESULTS

Characterization of the hAhR−YFP Fusion Protein. To confirm that the hAhR−YFP fusion resulted in no loss of function relative to the wild-type hAhR, hAhR−YFP and hAhR−FLAG were transiently coexpressed with XAP2 in COS-1 cells. Cytosol from cells expressing hAhR−FLAG or hAhR−YFP was isolated, and complexes were immunoprecipitated using anti-FLAG M2 affinity resin or anti-GFP antibody bound to protein G-sepharose, respectively. Immunoprecipitates were resolved by TSDS−PAGE, transferred to PVDF membrane, and visualized by Western blot (Figure 1A). Both hAhR−FLAG and hAhR−YFP coimmunoprecipitated hsp90 and XAP2, indicating that the fusion of YFP with the hAhR did not disrupt the ability to assemble into a core complex analogous to that of the wild-type hAhR. Further confirmation of the functionality of the hAhR−YFP fusion was obtained by examination of its ability to activate a DRE-driven luciferase reporter construct. COS-1 cells were transiently transfected with pGudLuc 6.1 (DRE-driven luciferase reporter construct) and either pEFV5/hAhR/FLAG or pEYFP/hAhR. Cells were treated with either DMSO (control) or 10 nM TCDD for 8 h, followed by assessment of luciferase activity (Figure 1B). The hAhR−YFP fusion demonstrated ligand induced luciferase activity, indicating that this receptor is functional. Although the total activity of hAhR−YFP appears to be less than hAhR−FLAG, the fold induction of activity for both receptors upon TCDD treatment is similar (Figure 1C). The variability seen in total activity may, at least in part, be due to differences in expression levels of hAhR−FLAG and hAhR−YFP.

Effect of XAP2 on Expression Levels of the Human and Mouse AhR in COS-1 Cells. Since XAP2 has previously been shown to increase the levels of cytosolic mAhR (*21*, *35*),

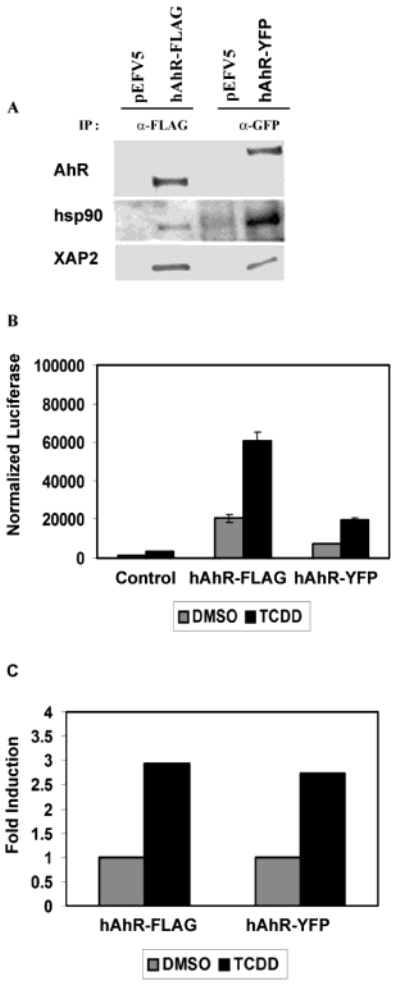

FIGURE 1: Both hAhR−YFP and hAhR−FLAG assemble into a tetrameric complex that mediates similar transcriptional activity. (A) COS-1 cells were cotransfected with pCI/XAP2 and either pEFV5/hAhR−FLAG or pEYFP/hAhR. hAhR−FLAG and hAhR−YFP were immunoprecipitated using anti-FLAG M2 agarose and anti-GFP antibody bound to Protein G agarose respectively and then separated by TSDS−PAGE. Proteins were transferred to PVDF membrane and visualized by Western blot analysis. (B) COS-1 cells in six-well plates were transfected with 10 ng of each receptor, 100 ng of pGudLuc 6.1, and 100 ng of pCMV-β gal. Cells were treated for 8 h with 10 nM TCDD or control solvent and lysed, and reporter assays were performed. (C) The data in B are represented as fold induction for hAhR−FLAG and hAhR−YFP.

we wanted to determine whether XAP2 has the same effect on the hAhR. COS-1 cells were grown in 100-mm culture dishes and transiently transfected with either pEFV5-hAhR (2 μg) or pcDNA3-mAhR (2 μg) and increasing amounts of pCI-XAP2. Approximately 18 h following transfection, cells were harvested and lysed, and cytosolic extracts were prepared and analyzed by TSDS−PAGE. Proteins were electroblotted to membrane and analyzed by Western blot analysis with anti-AhR and anti-XAP2 Abs, and then with [^{125}I]-labeled secondary Abs, followed by visualization with a phosphor imager. Increasing coexpression of XAP2 with the mAhR resulted in an increase in expression levels of receptor, while coexpression of XAP2 with the hAhR did not result in any significant change in the level of the hAhR (Figure 2) under these conditions. When XAP2 is expressed at relatively high levels with hAhR, a slight increase in hAhR levels can be seen (unpublished results). However, within the range of XAP2 concentrations tested in Figure 2, mAhR

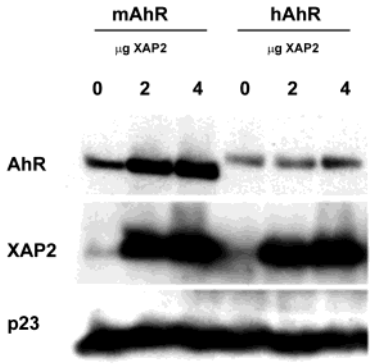

FIGURE 2: Effect of XAP2 on expression levels of the human and mouse Ah receptors in COS-1 cells. COS-1 cells in 100-mm dishes were transfected with 2 μg of pcDNA3/βmAhR or pEF/hAhR and increasing amounts of pCI/XAP2. Cytosol was extracted and separated by TSDS−PAGE. Proteins were transferred to PVDF membrane and analyzed by Western blot analysis.

levels increase, while hAhR levels do not increase significantly.

Comparison of the Subcellular Distribution of hAhR−YFP Relative to mAhR−YFP. In COS-1 cells, transient expression of mAhR−YFP has previously been shown to localize predominantly in the nucleus and is redistributed to the cytoplasm upon coexpression of XAP2 (*19*, *25*). To determine whether hAhR−YFP shows a similar localization pattern, COS-1 cells were transiently transfected with pEYFP/mAhR, pEYFP/mAhR + pCI/XAP2, pEYFP/hAhR, and pEYFP/hAhR + pCI/XAP2. Approximately 18 h following transfection, cells were directly visualized by fluorescence microscopy. As expected, mAhR−YFP localized largely in cell nuclei, and coexpression of XAP2 resulted in a distinct redistribution to the cytoplasm. In contrast to these results, the hAhR−YFP localized predominantly to cell cytoplasm, and coexpression of XAP2 did not affect this distribution pattern (Figure 3A,B). This would suggest that XAP2 plays a role in regulating the subcellular localization of mAhR, but perhaps not the hAhR.

Effect of XAP2 on Nucleocytoplasmic Shuttling of hAhR−YFP and mAhR−YFP. To examine for species-specific differences in nucleocytoplasmic shuttling of the hAhR and mAhR in the absence of ligand, the nuclear export inhibitor leptomycin B was utilized. COS-1 cells that were transiently transfected with pEYFP/mAhR, pEYFP/mAhR + pCI/XAP2, pEYFP/hAhR, and pEYFP/hAhR + pCI/XAP2 were treated with 10 nM leptomycin B. Transient expression of mAhR−YFP and XAP2 results in most of the mAhR−YFP localizing to the cytoplasm. Leptomycin B treatment does not result in distinct or complete nuclear accumulation of mAhR−YFP when XAP2 is coexpressed, indicating that XAP2 inhibits mAhR nucleocytoplasmic shuttling (Figure 3B). This suggests a possible mechanism for the increase in mAhR protein levels observed when XAP2 is coexpressed. In contrast, coexpression of hAhR−YFP and XAP2, followed by treatment with leptomycin B, resulted in rapid nuclear accumulation of hAhR−YFP, indicating that XAP2 is unable to inhibit nucleocytoplasmic shuttling of hAhR−YFP. This would suggest that XAP2 is capable of sequestering the mAhR in the cytoplasm, while the hAhR is unaffected by XAP2 coexpression.

Effect of XAP2−NLS Expression on mAhR and hAhR Subcellular Localization. Since XAP2 appeared to sequester

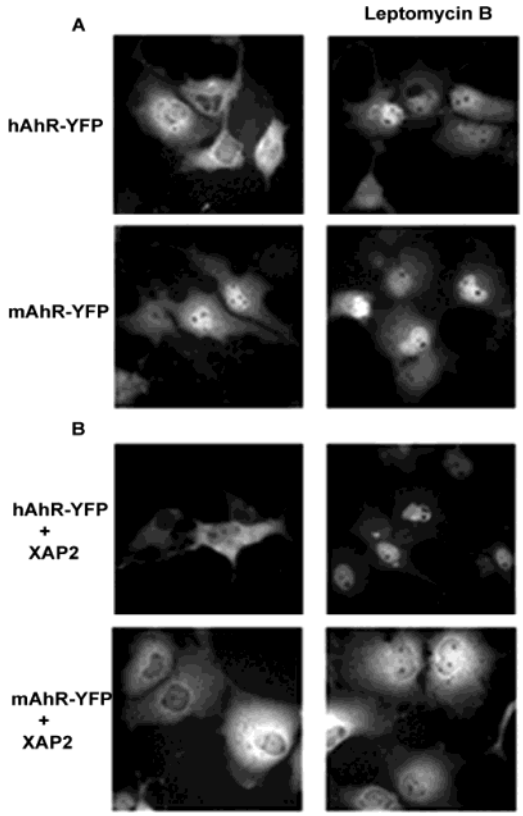

FIGURE 3: Influence of XAP2 on subcellular localization and nucleocytoplasmic shuttling of hAhR−YFP and mAhR−YFP in COS-1 cells. COS-1 cells in 6-well plates were transiently transfected with either 0.75 μg of pEYFP/mAhR or pEYFP/hAhR without or with 0.75 μg of pCI/XAP2. Cells were treated with 10 nM leptomycin B (LMB) for 1 h and visualized by fluorescence microscopy.

mAhR in the cytoplasm, but not the hAhR, we wanted to determine whether these receptors could enter the nucleus in the absence of ligand when XAP2 was targeted to the nucleus. A XAP2 construct with a NLS fusion at the carboxy terminal end was used to study whether this protein could drag the mAhR and hAhR to the nucleus. Coexpression of mAhR−YFP with XAP2−NLS resulted in cytoplasmic localization of mAhR−YFP, whereas coexpression of hAhR−YFP with XAP2−NLS resulted in partial nuclear localization of hAhR−YFP (Figure 4A). Upon treatment with leptomycin B (1 h), the nuclear accumulation of hAhR−YFP becomes more distinct, while mAhR remains cytoplasmic. The majority of XAP2−NLS appears to be in the nucleus, with a small portion in the cytoplasm, whereas XAP2 appears to be predominantly in the cytoplasm and a small portion is in the nucleus (Figure 4B), demonstrating that XAP2−NLS efficiently translocates to the nucleus.

We generated and used NLS mutants of mAhR and hAhR in a similar coexpression experiment with XAP2−NLS, to ensure that the only mechanism through which the receptors could enter the nucleus was by binding to XAP2−NLS. mAhR/K13A−YFP (a NLS point mutant of mAhR) is cytoplasmic when expressed in COS-1 cells and fails to accumulate in the nucleus even after leptomycin B treatment. When this construct was coexpressed with XAP2−NLS, it remained in the cytoplasm both before and after leptomycin B treatment, indicating that this receptor cannot be dragged into the nucleus by XAP2−NLS (Figure 4C). This suggests that mAhR, when bound to XAP2, undergoes some conformational change that prevents it from entering the nucleus. We generated three different NLS mutants of hAhR−YFP: pEYFP-hAhR/K14A (single mutation), pEYFP-hAhR/KRR14−16AAA (three point mutations), and pEYFP/hAhRΔ37−42 (deletion of six amino acids in the second half of the bipartite NLS). All three mutants are cytoplasmic when expressed in COS-1 cells (Figure 4C). When coexpressed with XAP2−NLS, hAhR/K14A−YFP and hAhR/KRR14−16AAA−YFP are predominantly cytoplasmic, whereas hAhR/Δ37−42−YFP shows a slightly diffuse distribution, showing nuclear localization in some cells. Upon treatment with leptomycin B for 1 h, all three NLS mutant receptors (when coexpressed with XAP2−NLS) accumulate in the nucleus, indicating that XAP2−NLS can drag these receptors into the nucleus. We have observed that when the NLS mutants of hAhR−YFP are expressed alone, they remain in the cytoplasm after 1 h of leptomycin B treatment, but begin to show some nuclear accumulation after 4 h of treatment (data not shown). Since the NLS mutants show distinct nuclear accumulation in the presence of XAP2−NLS and cytoplasmic localization in the absence of XAP2−NLS, after 1 h of leptomycin B treatment, it is clear that hAhR−YFP is being dragged into the nucleus by XAP2−NLS. Interestingly, mAhR/K13A−YFP is cytoplasmic in the absence and presence of XAP2−NLS, even after 4 h of leptomycin B treatment. These results suggest that XAP2 can remain bound to the hAhR upon translocation into the nucleus in the absence of ligand, while the mAhR appears incapable of translocating to the nucleus when complexed with XAP2.

To determine whether XAP2−NLS can drag ligand-bound mAhR and hAhR into the nucleus, we performed an experiment in which mAhR/K13A−YFP or hAhR/Δ37−42−YFP was coexpressed with XAP2−NLS and treated with 10 nM TCDD for 1 h, followed by leptomycin B treatment for 1 h. The NLS mutant receptors were used so that the ligand-bound receptor could enter the nucleus only through binding to XAP2−NLS, and not by ligand induced translocation. hAhR/Δ37−42−YFP accumulated in the nucleus following TCDD and leptomycin B treatment (Figure 4D), indicating that XAP2−NLS could drag this complex into the nucleus, and therefore, XAP2 can remain bound to the ligand-bound hAhR during nuclear translocation. Although hAhR/Δ37−42−YFP does appear to become somewhat diffuse in distribution in the presence of TCDD and leptomycin B, and in the absence of XAP2−NLS, it is distinctly nuclear in the presence of XAP2−NLS following treatment. This demonstrates that hAhR/Δ37−42−YFP is being dragged into the nucleus by XAP2−NLS. However, mAhR/K13A−YFP does not accumulate in the nucleus in the presence of XAP2−NLS and ligand, suggesting that XAP2−NLS cannot drag mAhR/K13A−YFP into the nucleus in either ligand-bound or ligand-free states. It is possible that XAP2 is not present in the ligand-bound mAhR complex that enters the nucleus. Co-immunoprecipitation experiments show that the nonmutant and NLS-mutant mouse and human receptors are capable of binding to XAP2 and XAP2−NLS in COS-1 cells (Figure 4E).

XAP2 Does Not Inhibit Importin β Binding to the hAhR. Previously, it has been shown that XAP2 inhibits importin β binding to the mAhR (*25*). In this report, this experiment

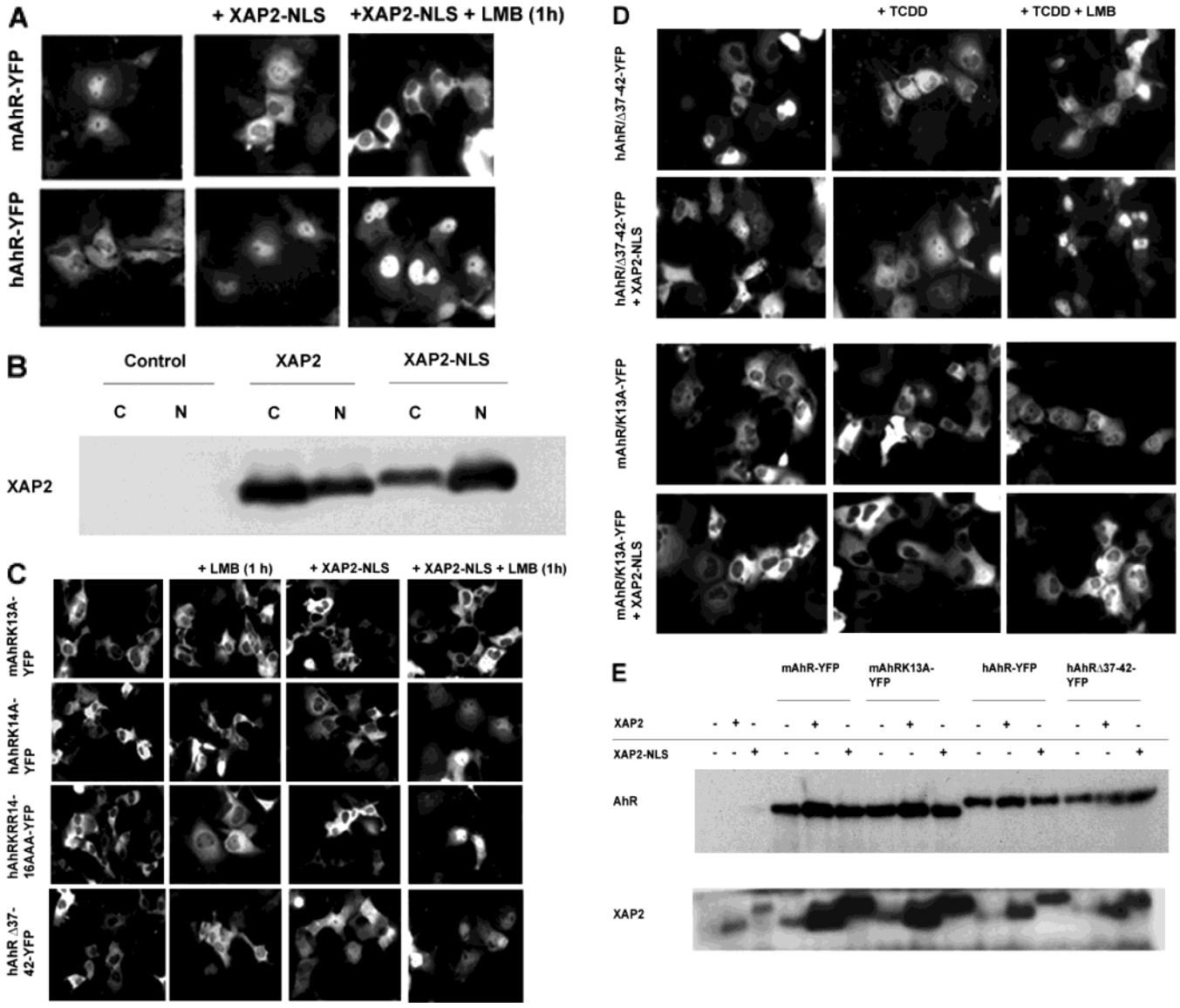

FIGURE 4: XAP2−NLS is capable of inducing nuclear translocation of the hAhR−YFP, while XAP2−NLS fails to induce mAhR−YFP nuclear uptake. (A) COS-1 cells were transfected with 0.75 μg of pEYFP/mAhR or pEYFP/hAhR without or with 0.75 μg of pCI/XAP2−FLAG-NLS. Cells were treated with 10 nM LMB for 1 h and then visualized by fluorescence microscopy. (B) COS-1 cells were transfected with 3 μg of pCI/XAP2 or pCI/XAP2/FLAG/NLS. Cells were harvested and cytosolic and nuclear extracts were prepared for each set of transfected cells. Equal amounts of protein from each extract were resolved by TSDS−PAGE, transferred to PVDF membrane and analyzed by Western blot as described under materials and methods. (C) COS-1 cells were transfected with pEYFP-/mAhR/K13A, pEYFP/hAhR/K14A, pEYFP/hAhR/KRR14−16AAA, or pEYFP/hAhR/Δ37−42, without or with 0.75 μg of pCI/XAP2/FLAG/NLS. Cells were treated with 10 nM leptomycin B for 1 h and visualized. (D) COS-1 cells were transfected with 0.75 μg of pEYFP/mAhR/K13A or pEYFP/hAhR/Δ37−42, without or with 0.75 μg of pCI/XAP2/FLAG/NLS. Cells were treated for 1 h with 10 nM TCDD followed by leptomycin B (10 nM) treatment for 1 h and visualized. (E) COS-1 cells were transfected with 3 μg of pEYFP/mAhR, pEYFP/mAhR/K13A, pEYFP/hAhR, or pEYFP/hAhR/Δ37−42 without or with 3 μg of pCI/XAP2 or pCI/XAP2/FLAG/NLS. Cells were harvested, cytosol was prepared, and immunoprecipitations were performed using an anti-GFP antibody as described under Experimental Procedures. Protein complexes were then resolved by TSDS−PAGE, transferred to PVDF membrane, and analyzed by Western blot.

was repeated with the hAhR under the same experimental conditions. hAhR−FLAG complexes were immunoprecipitated from COS-1 cells in which hAhR−FLAG was expressed alone or coexpressed with XAP2. An NLS mutant of hAhR−FLAG was also used as a control for importin binding specificity. These complexes were displaced from the anti-FLAG resin and then incubated with GST-importin β. This mixture was then incubated with glutathione sepharose, and complexes were finally eluted by using glutathione. The proteins were resolved by TSDS−PAGE, transferred to PVDF membrane, and the amount of hAhR, GST-Importin β, and XAP2 was determined. Human AhR complexes isolated from COS-1 cells in which XAP2 was cotransfected with hAhR−FLAG actually showed a small increase in importin β binding compared to hAhR isolated from transfected COS-1 cells where XAP2 was not coexpressed (Figure 5). This result is in contrast to a 40% inhibition of importin β binding to the mAhR isolated from cells cotransfected with XAP2 (*25*). This experiment indicates that XAP2 does not inhibit recognition of the hAhR's NLS by importin β. The NLS mutant hAhR/KRR14−16AAA/FLAG exhibits greatly reduced binding to GST-importin β compared to wild-type hAhR, indicating that importin β specifically recognizes hAhR's NLS.

hAhR Complexes Have Less XAP2 Associated with the Receptor than the mAhR Complex. To determine whether

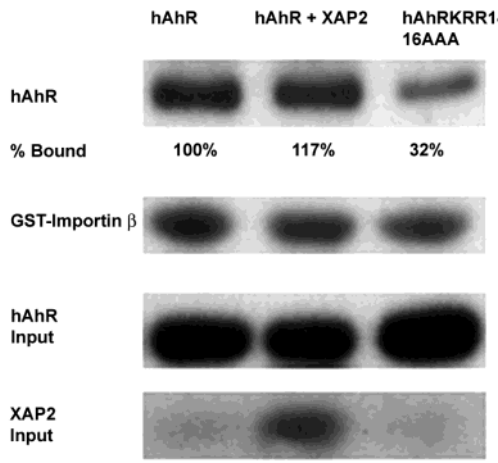

FIGURE 5: The presence of XAP2 in the hAhR complex does not inhibit importin β binding to the receptor's NLS. COS-1 cells were transfected with pCI/hAhR−FLAG, without or with pCI/XAP2, or pCI/hAhR−FLAG-KRR14−16AAA. Cytosol was prepared and treated with 10 nM TCDD or control solvent. Protein complexes were then immunoprecipitated with anti-FLAG M2 agarose and subsequently eluted using FLAG peptide. Eluted complexes were incubated with GST-Importin β and then bound to Glutathione sepharose. Finally, complexes were displaced using glutathione and then separated using TSDS−PAGE. Proteins were transferred to PVDF membrane and visualized by western blot.

the different effects of XAP2 on the mAhR and hAhR were due to differences in the amount of XAP2 present in the hAhR and mAhR complexes, a co-immunoprecipitation experiment was done. COS-1 cells were transfected with pcDNA3/mAhR/FLAG, or pCI/hAhR/FLAG and pCI/XAP2. For the hAhR transfections, more plasmid DNA (pCI/hAhR/FLAG) was transfected to achieve expression levels similar to the mAhR. FLAG immunoprecipitations were done with cytosol from transfected COS-1 cells and complexes were separated by TSDS−PAGE and transferred to PVDF membrane and probed for AhR, XAP2, and hsp90. The hAhR immunoprecipitations indicated that approximately 33% less XAP2 co-immunoprecipitated with hAhR−FLAG than with mAhR−FLAG, while the amount of hsp90 co-immunoprecipitated appeared similar between the two receptors. Although these results reflect differences in hAhR and mAhR complexes in vitro, it is possible that the lower amount of XAP2 in hAhR complex accounts for differences seen between mAhR and hAhR within a cell.

Effect of XAP2 on the Rate of Ligand-Induced Nuclear Accumulation of the Human AhR. XAP2 appears to have no effect on ligand-independent nucleocytoplasmic shuttling of the hAhR. We wanted to test whether XAP2 alters the rate of ligand-dependent translocation of the hAhR. COS-1 cells transfected with hAhR−YFP, with and without cotransfected XAP2, were treated with TCDD and the relative level of translocation was assessed by visual inspection at 15, 30, 60, and 180 min. An increase in the rate of translocation of hAhR−YFP after 15 min of TCDD treatment was detected in cells cotransfected with XAP2, with almost 30% of the cells scored displaying predominantly nuclear localization (Figure 7). In contrast, without cotransfected XAP2, hAhR−YFP did not show a significant level of nuclear localization in cells until after 30 min of TCDD treatment. These results suggest that the presence of high levels of XAP2 actually enhances the rate of hAhR translocation. Previous work by another group has shown that in HeLa cells, there is a delay

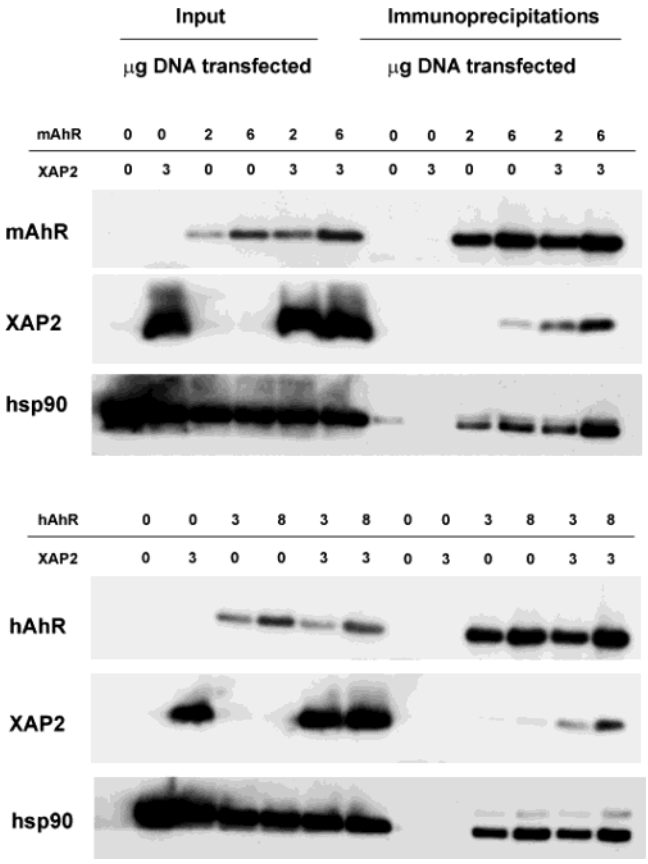

FIGURE 6: The hAhR complex is less stable than the mAhR complex. pcDNA3/mAhR−FLAG or pCI/hAhR−FLAG were cotransfected without and with XAP2 into COS-1 cells in 100 mM dishes. Cells were harvested 22 h post-transfection, and receptor complexes were immunoprecipitated from cytosol using anti-FLAG M2 resin. The precipitated complexes were washed and separated by tricine-SDS−PAGE. Western blot analysis was performed using antibodies against AhR, XAP2, and hsp90 and appropriate iodinated secondary antibodies. Band intensities were estimated using a gamma counter. For hsp90 Western blot, AhR blots were stripped and then reprobed for hsp90. The abbreviations are mR; mAhR, hR; hAhR, X; XAP2.

in nuclear translocation of liganded mAhR in the presence of cotransfected XAP2 (*20*). This experiment cannot, however, be done in COS-1 cells, because mAhR−YFP is predominantly nuclear in the absence of XAP2 and in the absence of ligand. Therefore, the ligand-induced nuclear translocation rate of mAhR−YFP in the absence of XAP2 cannot be measured and compared against the rate of translocation in the presence of XAP2. On the basis of the results of Kazlauskas et al. (*20*), for the mAhR, and our results in this report for the hAhR, there appears to be a difference in the role that XAP2 plays in ligand-induced nuclear translocation of the two receptors.

Effect of XAP2 on the Transactivation Potential of hAhR. Since XAP2 was capable of increasing the translocation rate of liganded hAhR, we wanted to test whether XAP2 has an effect on the transcriptional potential of hAhR. We have previously shown that XAP2 represses transcription by the mAhR (*25*). An increase in translocation rate of the hAhR would suggest that XAP2 may increase transcription by the hAhR. However, as shown in Figure 8, XAP2 actually represses transcription of a DRE driven luciferase reporter gene by hAhR, suggesting that XAP2 can influence hAhR negatively even after nuclear translocation.

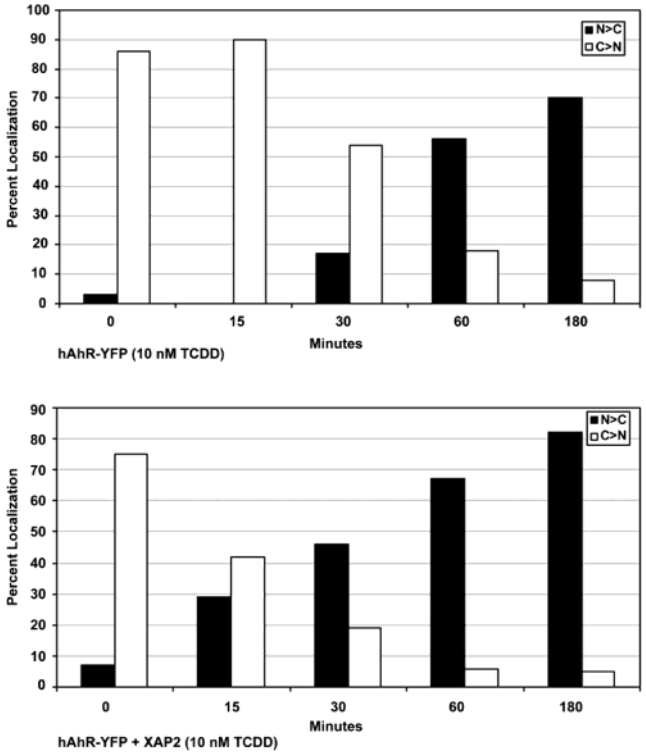

FIGURE 7: XAP2 increased the rate of ligand-mediated nuclear accumulation of the hAhR. COS-1 cells were transfected with 0.75 μg of pEYFP/hAhR without or with 0.75 μg of pCI/XAP2. Cells were treated with 10 nM TCDD and observed at the different times indicated. The number of cells showing nuclear localization versus the number of cells showing cytoplasmic localization were scored and plotted.

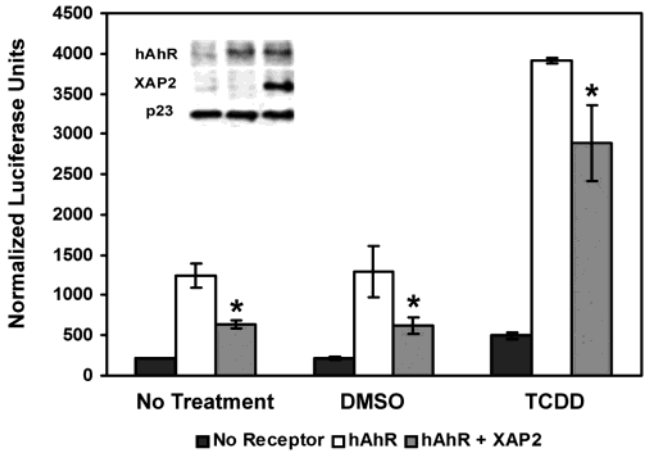

FIGURE 8: XAP2 represses hAhR mediated transcription. COS-1 cells were transfected in six-well plates with 50 ng of pCI/hAhR, 100 ng of pGudLuc6.1, 200 ng of pCI/XAP2 and pcDNA3 empty vector, to a total of 1.5 μg of DNA per well. Cells were dosed for 7.5 h, with 5 nM TCDD lysed, and luciferase and protein assays were performed on the lysates. An asterisk indicates a statistical difference from values obtained in the absence of XAP2 using an unpaired Student's t-test, in each treatment type. The p values for control, DMSO, and TCDD treated samples are 0.0032, 0.0026 and 0.0020, respectively. The error bars indicate standard deviation from the mean value.

DISCUSSION

A majority of studies that evaluate toxicity of AhR ligands are done using mouse models, and these data are extrapolated to estimate risk to humans. Since toxic endpoints are mediated through the AhR, differences between the mouse and human Ah receptors are important. Differences in biochemical properties of the receptors, such as ligand affinity, transcriptional activity, target gene specificity, and interactions with other proteins, could have an effect on the toxic endpoint that results from exposure to AhR ligands. There are significant differences between the amino acid sequences of the mouse and human Ah receptors. However, it remains to be determined whether these differences lead to important functional alterations. The hAhR has a molecular mass of ~105 kDa compared to ~95 kDa for the mAhR; this difference is due to a change in the position of a stop codon. In addition, there is only 58% amino acid sequence identity in the carboxyl terminal half of the protein between mAhR and hAhR. There have been relatively few studies that have examined the biochemical and transcriptional behavior of the hAhR. The human receptor is relatively less stable than the mouse receptor and requires molybdate in the homogenization buffer to stabilize the AhR/hsp90 interaction (*38*). It has also been shown that hAhR has a lower affinity for hsp90 binding as compared to the mAhR (*39*). In addition, the human receptor appears to have a lower affinity for ligand (*40*). However, it is important to note that all of these properties have been measured in vitro.

The AhR undergoes nucleocytoplasmic shuttling in the absence of ligand treatment (*22*, *23*, *41*). The relative amount of receptor in cytoplasm compared to the nucleus depends on the rate of nuclear import relative to the rate of nuclear export. mAhR is predominantly nuclear when expressed in COS-1 cells, and relocalizes to the cytoplasm when coexpressed with XAP2. XAP2 blocks nucleocytoplasmic shuttling of the mAhR (*25*, *42*). In contrast, hAhR localizes predominantly to the cytoplasm in COS-1 cells, and this localization is not altered by coexpression of XAP2. mAhR protein levels increase with increasing coexpression of XAP2, while hAhR protein levels do not increase significantly with coexpression of XAP2. This difference could, in part, be explained by XAP2's ability to sequester mAhR, but not the hAhR, to the cytoplasm, Recently, it was determined that an apparent mechanism by which XAP2 retained mAhR in the cytoplasm was due to XAP2 hindering importin β binding to the NLS of the mAhR (*25*). The proposed mechanism is that XAP2 binding to the mAhR results in an altered conformation of the bipartite NLS, which blocks importin β binding and subsequent nuclear translocation of the mAhR. In contrast, here we have determined that XAP2 does not hinder importin β binding to the NLS of the hAhR, but instead may actually slightly stimulate this binding. This is consistent with the observation that hAhR is not sequestered in the cytoplasm by XAP2; the conformation of hAhRs NLS may not be altered in a way similar to the mAhR upon binding to XAP2, and therefore XAP2 does not affect ligand-independent shuttling of the receptor.

Targeting XAP2 to the nucleus resulted in mAhR relocalizing to the cytoplasm, whereas hAhR was partially dragged to the nucleus (Figure 4). Leptomycin B treatment revealed that mAhR was not shuttling in the presence of XAP2−NLS, and the cytoplasmic localization of mAhR was due to nuclear exclusion and not due to an enhanced rate of nuclear export. This further demonstrates that the conformation of mAhR is altered when bound to XAP2 in such a way that it cannot enter the nucleus in a ligand-independent manner. In contrast, the hAhR enters the nucleus in the

presence of XAP2−NLS and in the absence of ligand; XAP2 is likely to be present in the hAhR complex that shuttles into the nucleus. The NLS mutants of mAhR and hAhR were used in coexpression experiments with XAP2−NLS to eliminate the possibility that the receptors could enter the nucleus by use of their own NLS. The NLS mutant of mAhR−YFP (mAhR/K13A−YFP) is not dragged into the nucleus, whereas the NLS mutants of hAhR−YFP are dragged into the nucleus by XAP2−NLS. Interestingly, while a single mutation in mAhR's NLS (K13A) was sufficient to cause nuclear exclusion of the receptor, a corresponding mutation (hAhR/K14A−YFP), triple mutations (hAhR/KRR14−16AAA−YFP), and a deletion (hAhR/Δ37−42−YFP) in hAhR were not sufficient to cause complete nuclear exclusion of hAhR. However, this difference was visible only after 4 h of leptomycin B treatment for both mAhR and hAhR mutant receptors (data not shown). Although the amino acid sequence near the NLS is well conserved between the mAhR and hAhR, the divergence in the behavior of the two receptors could be due to other differences elsewhere in the sequences, or due to an overall change in conformation around the NLS. Alternatively, there could be an NLS-independent mechanism through which the hAhR is transported to the nucleus, which does not occur in the case of the mAhR. hAhR/Δ37−42−YFP is also dragged into the nucleus by XAP2−NLS in the ligand-bound state (Figure 4C), whereas mAhR/K13A−YFP is not dragged into the nucleus by XAP2−NLS even in the presence of ligand. It is not yet clear why mAhR/K13A/YFP is unable to enter the nucleus even in the presence of ligand, but it is possible that XAP2 does not stay bound to the mAhR once mAhR is bound to ligand, and therefore XAP2−NLS cannot drag mAhR into the nucleus. Further experiments will have to be done to determine if this is the case.

The inability of XAP2 to inhibit ligand-independent shuttling of the hAhR as well as the ability of XAP2−NLS to drag the hAhR into the nucleus suggests that the receptor shuttles with both hsp90 and XAP2 in the complex. Therefore, XAP2 may have some function in the nucleus after it translocates into the nucleus as part of the hAhR complex. It was shown previously that XAP2 is capable of hindering mAhR's binding to importin β, and that this may be the mechanism through which XAP2 sequesters mAhR in the cytoplasm (*25*). This mechanism would be dependent on the NLS of mAhR. However, XAP2−NLS is unable to drag mAhR/K13A−YFP into the nucleus, indicating that a mechanism that is independent of the mAhR's NLS is responsible for cytoplasmic sequestering of mAhR by XAP2. This could include tethering or docking of the mAhR to structures in the cytoplasm. This has previously been suggested by another group (*42*). In their experiments, XAP2 was unable to sequester mAhR in the cytoplasm in HeLa cells, in the presence of cytochalasin B (an inhibitor of actin polymerization), and actin was shown to co-immunoprecipitate with mAhR and XAP2. It was therefore suggested that XAP2 mediates the interaction between mAhR and actin, and this interaction is responsible for retaining the mAhR in the cytoplasm. Thus, two mechanisms may be involved in the XAP2-mediated cytoplasmic retention of the mAhR in the cytoplasm.

XAP2 appears to enhance ligand-dependent translocation of the hAhR (Figure 7), and this is consistent with the observation that XAP2 slightly enhances importin β binding by the hAhR's NLS. Since XAP2 increases hAhR's translocation, and appears to be present in the hAhR complex that translocates to the nucleus, it was expected to enhance hAhR's transcriptional activity. However, as shown in Figure 8, XAP2 represses transcriptional activity of the hAhR in a DRE-driven reporter assay. This repression has been reported previously for the mAhR (*25*). It is important to note that these reporter assays were carried out at saturating ligand concentrations, and the magnitude of repression mediated by XAP2 may be greater at lower ligand concentrations. Therefore, although the mAhR and hAhR behave differently in terms of nuclear import and export in the presence of XAP2, the transcriptional activity of both receptors is repressed by XAP2. The mechanism through which this repression is mediated is not known, and could be different for the two receptors. The mAhR's transcriptional activity could be repressed because XAP2 retards translocation of the ligand-bound complex into the nucleus. In constrast, hAhR may be repressed because XAP2 inhibits a step after ligand binding and nuclear translocation. On the basis of the data from this study, a model for ligand-independent shuttling and ligand-dependent nuclear translocation for mAhR and hAhR is shown in Figure 9. While mAhR can enter the nucleus only when XAP2 is absent from the receptor complex, hAhR can enter the nucleus with XAP2 present in the receptor complex in both the ligand-bound and ligand-free states.

In summary, this report shows for the first time that XAP2 regulates the biochemical behavior of mAhR and hAhR differently. In COS-1 cells, XAP2 enhances mAhR levels but not hAhR levels and inhibits nucleocytoplasmic shuttling of the mAhR, but not of the hAhR. XAP2 appears to be present in the hAhR complex that shuttles into the nucleus in the absence of ligand and does not hinder β-importin binding by the hAhR, while mAhR cannot shuttle into the nucleus in the presence of XAP2 and β-importin binding by the mAhR is inhibited by XAP2. XAP2 appears to be present in the ligand-bound hAhR complex that translocates into the nucleus, but not in the analogous ligand-bound mAhR complex. Although the exact mechanism is not yet clear, it is still possible that XAP2 is not present in the nuclear ligand-bound mAhR complex. Further experiments will have to be conducted to test this hypothesis. The hAhR complex appears to have less XAP2 than the mAhR complex in vitro, and this may reflect a difference in the amount of XAP2 present in mAhR and hAhR complexes in cells, which in turn could contribute to differences seen between mAhR and hAhR. Interestingly, while XAP2 appears to enhance the ligand-bound hAhR's translocation into the nucleus, it represses transcriptional activation by the hAhR. It is possible that XAP2 inhibits AhR/ARNT heterodimer formation in the nucleus, and this is supported by the fact that XAP2 is not found associated with the AhR/ARNT heterodimer either in vitro or in Hepa-1 nuclear extracts (*18*). XAP2 also represses transcriptional activity of the mAhR (*25*). In mouse tissues/organs where XAP2 levels are high, the mouse AhR may behave differently from the human AhR in the corresponding human tissues/organs. While the transcriptional potential of both receptors in corresponding tissues would be affected negatively by XAP2, other activities of the receptors may differ. While this report characterizes the differences in

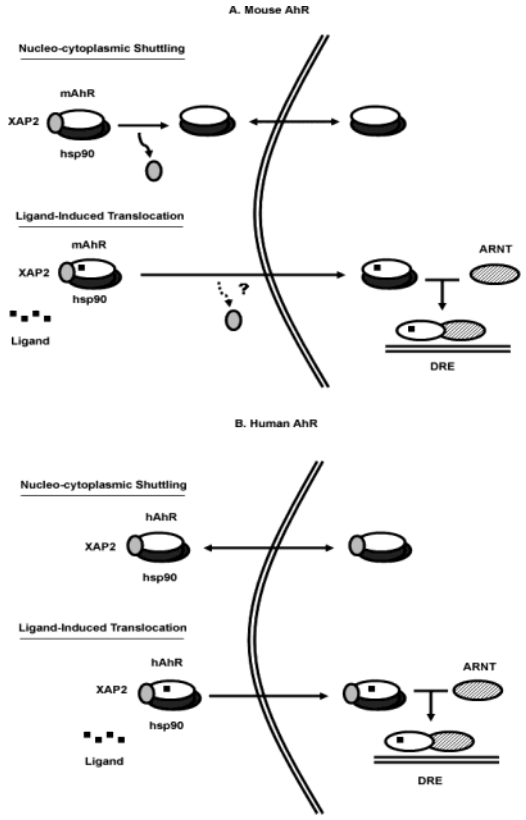

FIGURE 9: Model of XAP2-mediated regulation of (A) mAhR and (B) hAhR. XAP2 represses the ability of mAhR to enter the nucleus in the absence of ligand, whereas hAhR can enter the nucleus with XAP2 in the ligand-free state. In the presence of ligand, XAP2 remains bound the hAhR; in constrast, XAP2 dissociates from the mAhR prior to nuclear translocation.

modulation of mAhR and hAhR by XAP2, there are a number of other differences between the mAhR and hAhR that remain to be characterized, such as ligand affinity in vivo, transcriptional activity at different target gene promoters, and target gene specificity. Significant differences in any of these properties could result in an overall difference in the response to TCDD-induced activity, including toxic endpoints. Such differences would be an important consideration in evaluating the risk of exposure to AhR ligands for humans. Finally, the fact that there is a significant difference between the mouse and human Ah receptors, raises the possibility that other transcription factors may exhibit similar species specific variations.

ACKNOWLEDGMENT

We thank Drs. Oliver Hankinson, Mike Denison, Ed Seto, and Steve Adam for vectors and Dr. David Toft for the p23 antibody JJ5.

REFERENCES

1. Huff, J. E., Moore, J. A., Saracci, R., and Tomatis, L. (1980) *Environ. Health Perspect. 36*, 221−40.
2. Burbach, K. M., Poland, A., and Bradfield, C. A. (1992) *Proc. Natl. Acad. Sci. U.S.A. 89*, 8185−9.
3. Gu, Y. Z., Hogenesch, J. B., and Bradfield, C. A. (2000) *Annu. Rev. Pharmacol. Toxicol. 40*, 519−61.
4. Schmidt, J. V., Su, G. H., Reddy, J. K., Simon, M. C., and Bradfield, C. A. (1996) *Proc. Natl. Acad. Sci. U.S.A. 93*, 6731−6.
5. Lahvis, G. P., Lindell, S. L., Thomas, R. S., McCuskey, R. S., Murphy, C., Glover, E., Bentz, M., Southard, J., and Bradfield, C. A. (2000) *Proc. Natl. Acad. Sci. U.S.A. 97*, 10442−7.
6. Petrulis, J. R., and Perdew, G. H. (2002) *Chem. Biol. Interact. 141*, 25−40.
7. Reyes, H., Reisz-Porszasz, S., and Hankinson, O. (1992) *Science 256*, 1193−5.
8. Wu, L., and Whitlock, J. P., Jr. (1992) *Proc. Natl. Acad. Sci. U.S.A. 89*, 4811−5.
9. Zhang, L., Savas, U., Alexander, D. L., and Jefcoate, C. R. (1998) *J. Biol. Chem. 273*, 5174−83.
10. Bock, K. W., Gschaidmeier, H., Heel, H., Lehmkoster, T., Munzel, P. A., Raschko, F., and Bock-Hennig, B. (1998) *Adv. Enzyme Regul. 38*, 207−22.
11. Rushmore, T. H., and Pickett, C. B. (1990) *J. Biol. Chem. 265*, 14648−53.
12. Carver, L. A., and Bradfield, C. A. (1997) *J. Biol. Chem. 272*, 11452−6.
13. Ma, Q., and Whitlock, J. P., Jr. (1997) *J. Biol. Chem. 272*, 8878−84.
14. Meyer, B. K., Pray-Grant, M. G., Vanden Heuvel, J. P., and Perdew, G. H. (1998) *Mol. Cell Biol. 18*, 978−88.
15. Carver, L. A., Jackiw, V., and Bradfield, C. A. (1994) *J. Biol. Chem. 269*, 30109−12.
16. Antonsson, C., Whitelaw, M. L., McGuire, J., Gustafsson, J. A., and Poellinger, L. (1995) *Mol. Cell Biol. 15*, 756−65.
17. Whitelaw, M. L., McGuire, J., Picard, D., Gustafsson, J. A., and Poellinger, L. (1995) *Proc. Natl. Acad. Sci. U.S.A. 92*, 4437−41.
18. Meyer, B. K., and Perdew, G. H. (1999) *Biochemistry 38*, 8907−17.
19. Petrulis, J. R., Hord, N. G., and Perdew, G. H. (2000) *J. Biol. Chem. 275*, 37448−53.
20. Kazlauskas, A., Poellinger, L., and Pongratz, I. (2000) *J. Biol. Chem. 275*, 41317−24.
21. LaPres, J. J., Glover, E., Dunham, E. E., Bunger, M. K., and Bradfield, C. A. (2000) *J. Biol. Chem. 275*, 6153−9.
22. Ikuta, T., Eguchi, H., Tachibana, T., Yoneda, Y., and Kawajiri, K. (1998) *J. Biol. Chem. 273*, 2895−904.
23. Ikuta, T., Tachibana, T., Watanabe, J., Yoshida, M., Yoneda, Y., and Kawajiri, K. (2000) *J. Biochem. (Tokyo) 127*, 503−9.
24. Pollenz, R. S., and Barbour, E. R. (2000) *Mol. Cell Biol. 20*, 6095−104.
25. Petrulis, J. R., Kusnadi, A., Ramadoss, P., Hollingshead, B., and Perdew, G. H. (2003) *J. Biol. Chem. 278*, 2677−85.
26. Poland, A., and Glover, E. (1990) *Mol. Pharmacol. 38*, 306−12.
27. Poland, A., Palen, D., and Glover, E. (1994) *Mol. Pharmacol. 46*, 915−21.
28. Pohjanvirta, R., Wong, J. M., Li, W., Harper, P. A., Tuomisto, J., and Okey, A. B. (1998) *Mol. Pharmacol. 54*, 86−93.
29. Korkalainen, M., Tuomisto, J., and Pohjanvirta, R. (2000) *Biochem. Biophys. Res. Commun. 273*, 272−81.
30. Dolwick, K. M., Schmidt, J. V., Carver, L. A., Swanson, H. I., and Bradfield, C. A. (1993) *Mol. Pharmacol. 44*, 911−7.
31. Fukunaga, B. N., and Hankinson, O. (1996) *J. Biol. Chem. 271*, 3743−9.
32. Kumar, M. B., Ramadoss, P., Reen, R. K., Vanden Heuvel, J. P., and Perdew, G. H. (2001) *J. Biol. Chem. 276*, 42302−10.
33. Makarova, O., Kamberov, E., and Margolis, B. (2000) *Biotechniques 29*, 970−2.
34. Prieve, M. G., Guttridge, K. L., Munguia, J., and Waterman, M. L. (1998) *Mol. Cell Biol. 18*, 4819−32.
35. Meyer, B. K., Petrulis, J. R., and Perdew, G. H. (2000) *Cell Stress Chaperones 5*, 243−54.
36. Perdew, G. H., Abbott, B., and Stanker, L. H. (1995) *Hybridoma 14*, 279−83.
37. Perdew, G. H., Hord, N., Hollenback, C. E., and Welsh, M. J. (1993) *Exp. Cell Res. 209*, 350−6.
38. Manchester, D. K., Gordon, S. K., Golas, C. L., Roberts, E. A., and Okey, A. B. (1987) *Cancer Res. 47*, 4861−8.
39. Hogenesch, J. B., Chan, W. K., Jackiw, V. H., Brown, R. C., Gu, Y. Z., Pray-Grant, M., Perdew, G. H., and Bradfield, C. A. (1997) *J. Biol. Chem. 272*, 8581−93.
40. Harper, P. A., Golas, C. L., and Okey, A. B. (1988) *Cancer Res. 48*, 2388−95.
41. Richter, C. A., Tillitt, D. E., and Hannink, M. (2001) *Arch. Biochem. Biophys. 389*, 207−17.
42. Berg, P., and Pongratz, I. (2002) *J. Biol. Chem. 277*, 32310−9.

BI035827V